Polarization imaging reflectometry in the wild - supplemental material

JÉRÉMY RIVIERE, Imperial College London
ILYA RESHETOUSKI, Imperial College London
LUKA FILIPI, Imperial College London
ABHIJEET GHOSH, Imperial College London

ACM Reference format:
Jérémy Riviere, Ilya Reshetouski, Luka Filipi, and Abhijeet Ghosh. 2017. Polarization imaging reflectometry in the wild - supplemental material. *ACM Trans. Graph.* 36, 6, Article 206 (November 2017), 4 pages.
https://doi.org/10.1145/3130800.3130894

1 SYMBOLS AND ABBREVIATIONS

TRS Transmitted Radiance Sinusoid
DOLP Degree of Linear Polarization
$\boldsymbol{\rho_d}$ Diffuse albedo
$\boldsymbol{f_r(\sigma;\eta;\vec{\omega_i},\vec{\omega_o})}$ Specular BRDF
$\boldsymbol{\vec{n}}$ Surface normal
$\boldsymbol{L_i(\vec{\omega_i})}$ Incoming radiance
$\boldsymbol{\theta_B}$ Brewster angle
$\boldsymbol{E_\parallel}$ Unit vector parallel to the plane of incidence
$\boldsymbol{E_\perp}$ Unit vector perpendicular to the plane of incidence
$\boldsymbol{R_\parallel}$ Reflectance of p-polarized light
$\boldsymbol{R_\perp}$ Reflectance of s-polarized light
$\boldsymbol{\delta}$ Phase retardation between the orthogonally projected images of the electric vector
$\boldsymbol{I_{max}}$ Maximum intensity of the Transmitted Radiance Sinusoid (TRS)
$\boldsymbol{I_{min}}$ Minimum intensity of the Transmitted Radiance Sinusoid (TRS)
$\boldsymbol{\phi}$ Angular phase of the TRS
$\boldsymbol{\phi_o}$ Angle of rotation of the polariser with respect to camera coordinates
$\boldsymbol{x_{i,o,ref}}$ Subscript indicates input (i), output (o) or reflection (ref), where x can be any symbol listed thereafter
$\boldsymbol{\mathcal{P}}$ Degree of Linear Polarization (DOLP)
$\boldsymbol{\psi}$ Angle of polarization expressed in local coordinates
$\boldsymbol{\chi}$ Ellipticity angle expressed in local coordinates
$\boldsymbol{\vec{\omega}}$ Unit direction in spherical coordinates ($\vec{\omega} = (\theta, \phi)$)
$\boldsymbol{s}$ Stokes vector ($s = [s_0\ s_1\ s_2\ s_3]^T$)

2 BACKGROUND - POLARIZATION

2.1 Stokes parameters and Mueller Calculus

The polarization state of light can be formalized by Stokes parameters, expressed as a 4-vector $s = [s_0, s_1, s_2, s_3]^T$, where s_0 is the power of the incident beam, s_1 and s_2 respectively the power of 0° and +45° linear polarization and s_3 the power of right circular polarization. Each of these components are related in the general case to light intensity ($L(\vec{\omega})$), degree of polarization ($\mathcal{P}$) and polarization ellipse (Figure 1).

Upon reflection off a surface, the incident polarization state of light is altered according to Mueller calculus [Collett 2005]:

$$s_{ref} = M_{rot}(\phi) M_{ref}(\theta_i; \delta; \vec{n}) M_{rot}(\psi_i) s_i \tag{1}$$

Here, $M_{rot}(\psi_i)$ rotates the incident Stokes vector s_i into a canonical frame of reference (plane of incidence), and $M_{rot}(\phi)$ rotates the reflected light into the camera's reference frame. $M_{ref}(\theta_i; \delta; \vec{n})$ is

0730-0301/2017/11-ART206 $15.00
https://doi.org/10.1145/3130800.3130894

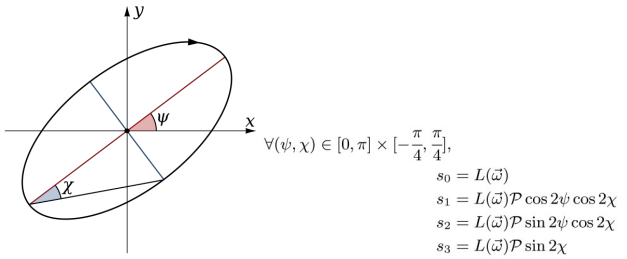

Fig. 1. *Polarization ellipse:* ψ is the orientation angle of the ellipse and corresponds to the angle of polarization of the beam. χ is the ellipticity angle which accounts for how elliptically polarized the beam is. The vectors $\vec{x}$ and $\vec{y}$ form an orthonormal basis in the plane orthogonal to the direction of propagation.

the concatenation of the Mueller matrices of a linear diattenuator, also referred to as Mueller reflection matrix, and a linear retarder of phase δ:

$$M_{ref} = \begin{bmatrix} \frac{R_\parallel + R_\perp}{2} & \frac{R_\perp - R_\parallel}{2} & 0 & 0 \\ \frac{R_\perp - R_\parallel}{2} & \frac{R_\parallel + R_\perp}{2} & 0 & 0 \\ 0 & 0 & \sqrt{R_\parallel R_\perp}\cos\delta & \sqrt{R_\parallel R_\perp}\sin\delta \\ 0 & 0 & -\sqrt{R_\parallel R_\perp}\sin\delta & \sqrt{R_\parallel R_\perp}\cos\delta \end{bmatrix} \tag{2}$$

$R_\perp$ and $R_\parallel$ in Equation (2) represent the relative amounts of reflected s-polarized (resp. p-polarized) light as predicted by Fresnel equations. δ is the relative phase between the s- and p-polarized components. For dielectric materials, $\delta = 180°$ for any angle of incidence before the Brewster angle θ_B (where index of refraction $\eta = \tan\theta_B$), and $\delta = 0°$ beyond the Brewster angle.

The Mueller matrix of rotation M_{rot} is defined as:

$$M_{rot}(\alpha) = \begin{bmatrix} 1 & 0 & 0 & 0 \\ 0 & \cos 2\alpha & -\sin 2\alpha & 0 \\ 0 & \sin 2\alpha & \cos 2\alpha & 0 \\ 0 & 0 & 0 & 1 \end{bmatrix} \tag{3}$$

We also define the Mueller matrix for a linear polarizer rotated at an angle ϕ_o with respect to the observation's coordinate system as:

$$M_o(\phi_o) = \frac{1}{2}\begin{bmatrix} 1 & \cos 2\phi_o & \sin 2\phi_o & 0 \\ \cos 2\phi_o & \cos^2 2\phi_o & \cos 2\phi_o \sin 2\phi_o & 0 \\ \sin 2\phi_o & \cos 2\phi_o \sin 2\phi_o & \sin^2 2\phi_o & 0 \\ 0 & 0 & 0 & 0 \end{bmatrix} \tag{4}$$

Light in outdoor environments due to the sky is either unpolarized (on a cloudy day) or partially linearly polarized in the general case.

Hence for such illumination, we only need to measure the first three components of the Stokes vector. This can be done by rotating a linear polarizer in front of a camera at three or more different orientations. Of particular interest to us in this work is analyzing the intensity of light reflected off regular planar surfaces as seen through a linear polarizer, which can be expressed with Mueller calculus as: $s_o(\phi_o) = M_o(\phi_o)s_{ref}$. Orienting a linear polarizer at 0°, 45° and 90° then allows us to compute the first three elements of the reflected Stokes vector:

$$\begin{aligned} s_{ref,0} &= s_{o,0}(0^\circ) + s_{o,0}(90^\circ) \\ s_{ref,1} &= s_{o,0}(0^\circ) - s_{o,0}(90^\circ) \\ s_{ref,2} &= 2 * s_{o,0}(45^\circ) - s_{ref,0} \end{aligned} \tag{5}$$

Note that Equation (1) holds for pure specular reflection only. Most real world materials also exhibit diffuse and rough specular reflection. We can account for rough specular reflections by modeling the surface with a microfacet BRDF where each microfacet behaves as per Equation (1). The resulting Stokes vector can then be computed as:

$$s_o(\vec{\omega}_o) = \int_\Omega \left(\frac{\boldsymbol{\rho_d}}{\pi} + f_r(\boldsymbol{\sigma};\boldsymbol{\eta};\vec{\omega}_i,\vec{\omega}_o) s_{ref}(\vec{\omega}_i) \right) L_i(\vec{\omega}_i)(\vec{\boldsymbol{n}} \cdot \vec{\omega}_i) d\vec{\omega}_i \tag{6}$$

Equation (6) is our complete image formation model, where we model $f_r(\boldsymbol{\sigma};\boldsymbol{\eta};\vec{\omega}_i,\vec{\omega}_o)$ as a Cook-Torrance microfacet BRDF [1982] with a GGX distribution [Walter et al. 2007]. The specular BRDF $f_r(\boldsymbol{\sigma};\boldsymbol{\eta};\vec{\omega}_i,\vec{\omega}_o)$ forms a narrow lobe around the reflection vector, within which the incident polarization can be assumed constant, as the polarization field typically varies smoothly over the sky [Können 1985]. Our goal is to recover the four parameters of diffuse albedo ($\boldsymbol{\rho_d}$), index of refraction ($\boldsymbol{\eta}$), surface normal ($\vec{\boldsymbol{n}}$) and specular roughness ($\boldsymbol{\sigma}$) from observations of $s_o(\vec{\omega}_o)$ under natural outdoors illumination.

3 TRANSMITTED RADIANCE SINUSOID

A known method for shape from polarization (unpolarized illumination assumption) is to consider the intensity profile of reflected light passing through a linear polarizer, which has the form of a phase-shifted sinusoid (Figure 3) of phase ϕ, with minimum and maximum amplitudes denoted as I_{min} and I_{max} respectively (consider for now that there is no diffuse component):

$$\begin{aligned} I(\phi_o) &= \frac{I_{max} + I_{min}}{2} + \frac{I_{max} - I_{min}}{2} \cos\left(2(\phi_o - \phi)\right) \\ \text{where } I_{max} &= L_i(\vec{\omega}_i)\frac{R_\perp}{2} \\ I_{min} &= L_i(\vec{\omega}_i)\frac{R_\parallel}{2} \end{aligned} \tag{7}$$

Equation (7) can be derived from Mueller calculus by considering the intensity of reflected light observed through a linear polarizer rotated at an angle ϕ_o. Mathematically, this is expressed as the dot product of the first row of Equation (4) with s_{ref}, where $s_{ref} = L_i(\vec{\omega}_i)\left[\frac{R_\perp + R_\parallel}{2}, \frac{R_\perp - R_\parallel}{2}\cos 2\phi, \frac{R_\perp - R_\perp}{2}\sin 2\phi, 0\right]^T$ for unpolarized incident illumination.

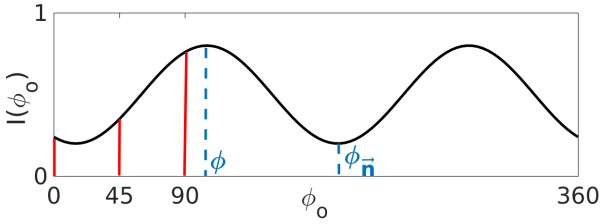

Fig. 3. The intensity profile through a linear polarizer has the form of a phase-shifted sinusoid of phase ϕ, which can be measured with only three measurements (red lines) at 0, 45, and 90°.

The phase ϕ and the I_{min} and I_{max} amplitudes of the TRS can then be recovered with just three measurements, e.g., with the polarizer at 0°, 45° and 90° orientations. Previous work [Huynh et al. 2010; Kadambi et al. 2015; Miyazaki et al. 2012] has shown the phase to be directly related to the azimuth $\phi_{\vec{n}}$ of the surface normal as $\phi_{\vec{n}} = \phi + \pi/2$. We found however that this holds true in principle only when the incident illumination has no linear polarization component. Under partial linear polarization, the expression for the reflected Stokes vector is more complex:

$$\begin{aligned} s_{ref} &= M_{rot}(\phi) M_{ref}(\theta_i;\delta;\vec{n}) s_i \\ &= L_i(\vec{\omega}_i) \begin{bmatrix} \frac{R_\perp + R_\parallel}{2} + \mathcal{P}_i \frac{R_\perp - R_\parallel}{2} \cos 2\psi_i \\ \frac{R_\perp - R_\parallel}{2} \cos 2\phi + \mathcal{P}_i * A \\ \frac{R_\perp - R_\parallel}{2} \sin 2\phi + \mathcal{P}_i * B \\ -\mathcal{P}_i \sqrt{R_\perp R_\parallel} \sin 2\psi_i \sin\delta \end{bmatrix} \end{aligned} \tag{8}$$

where

$$A = \frac{R_\perp + R_\parallel}{2} \cos 2\phi \cos 2\psi_i - \sqrt{R_\perp R_\parallel} \sin 2\phi sin2\psi_i \cos\delta$$

$$B = \frac{R_\perp + R_\parallel}{2} \sin 2\phi \cos 2\psi_i + \sqrt{R_\perp R_\parallel} \cos 2\phi sin2\psi_i \cos\delta$$

The corresponding expression for the TRS under partial linear polarization is then:

$$\begin{aligned} I(\phi_o) = \frac{I_\perp + I_\parallel}{2} + \frac{I_\perp - I_\parallel}{2} \cos\left(2(\phi_o - \phi)\right) \\ - L_i(\vec{\omega}_i) \frac{\mathcal{P}_i \sqrt{R_\parallel R_\perp} \cos\delta \sin 2\psi_i}{2} \sin\left(2(\phi_o - \phi)\right), \end{aligned} \tag{9}$$

where we define $I_\perp = L_i(\vec{\omega}_i)\frac{(1 + \mathcal{P}_i \cos 2\psi_i)R_\perp}{2}$, and $I_\parallel = L_i(\vec{\omega}_i)\frac{(1 - \mathcal{P}_i \cos 2\psi_i)R_\parallel}{2}$.

It is interesting to note that the above expression is somewhat similar to Equation (7) modulo the extra sinusoid term[1]. From Equation (9), we derive three special cases to connect the expression of the TRS under partial linear polarization back to the well-known expression under unpolarized incident illumination (Equation (7)):

[1]Note that we defined $I_\perp$ and $I_\parallel$ instead of I_{max} and I_{min} as $I_\parallel$ could be greater than $I_\perp$ depending on the sign of $\cos 2\psi_i$.

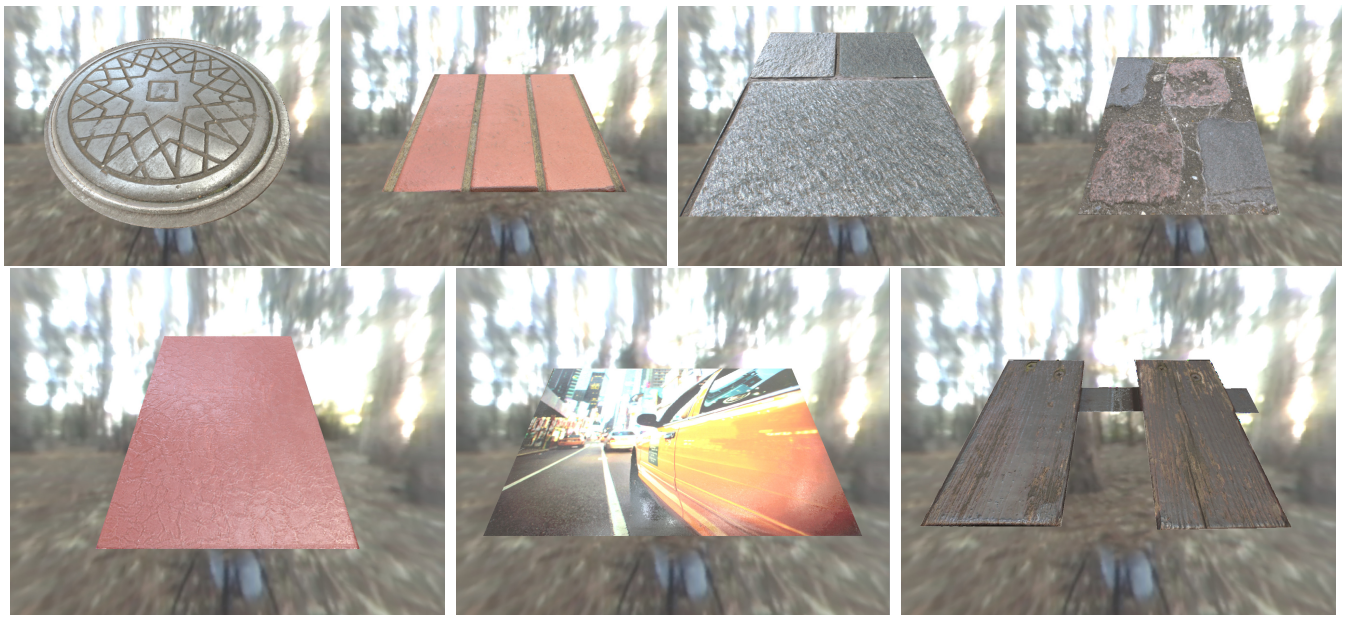

Fig. 2. Rendering of acquired samples (primary setup) in Eucalyptus Grove.

(1) At the Brewster angle, dielectrics completely transmit the component of light parallel to the plane of incidence, i.e. $R_{\parallel} = 0$. The extra sinusoid term thus vanishes and we obtain measurements at the Brewster angle that behave as if the incident illumination were unpolarized.
(2) Under horizontal or vertical polarization, i.e. $\psi_i = 0°$ (resp. 90°), $\sin 2\psi_i = 0$ also simplifying Equation (9) back to an expression of the same form as that assuming unpolarized illumination.

In these particular cases, the expression for the TRS is then, adding back the diffuse component (I_d):

$$I(\phi_o) = \frac{I_d}{2} + \frac{I_\perp + I_\parallel}{2} + \frac{I_\perp - I_\parallel}{2}\cos\left(2(\phi_o - \phi)\right)$$
$$\text{where } I_\perp = L_i(\vec{\omega}_i)\frac{(1 + \mathcal{P}_i \cos 2\psi_i)R_\perp}{2} \tag{10}$$
$$I_\parallel = L_i(\vec{\omega}_i)\frac{(1 - \mathcal{P}_i \cos 2\psi_i)R_\parallel}{2}$$

While mathematically it is possible for $I_\parallel$ to be greater than $I_\perp$ in Equation (10), it does not happen in practice with our near-Brewster measurements and hence does not adversely affect the phase (ϕ) computation. An example of this is vertically polarized light (max 80% DOP) at the Brewster angle (during sunrise or sunset). While there is no incident horizontal polarization signal and hence no perpendicular polarization on reflection, the strong vertical incident polarization is in-plane and does not reflect due to Fresnel effects. Now the only reflection that happens is due to the 20% unpolarized component of incident light which again results in only its perpendicular component reflecting with its parallel component transmitting.

4 PLANAR, DIELECTRIC ASSUMPTION

While our analysis makes the assumption of dielectric material, we show our method to work quite well in practice on dielectric-metal composite surfaces such as the cast-iron drain cover. The globally planar surface assumption is consistent with many recent SVBRDF capture methods e.g., [Aittala et al. 2016, 2013, 2015]. However, we demonstrate good qualitative results with significant surface normal variation in many of our measured samples, with low quantitative error compared to controlled measurements demonstrated for the red-book sample.

5 INDEX OF REFRACTION ESTIMATION

Given that the chart casing is made of plastic with a known index of refraction $\eta_{chart} = 1.46$. We then compute the scale factor between the plastic casing's measured diffuse subtracted maximum intensity and the pre-computed $R_{\perp,real}$. For lack of measurement device capable of accurately measuring the index of refraction of the colour chart's casing in our laboratory, we borrow the value of η_{chart} from online sources [Pixel and Poly 2017]. This is in line with prior work on skin reflectance [Donner and Jensen 2006; Ghosh et al. 2008] and Shape From Polarisation [Atkinson and Hancock 2006; Kadambi et al. 2015] which have shown the index of refraction to have a very marginal impact on reflection from dielectrics.

For further validation of index of refraction estimation, we compared our estimates for the canvas print surface to known values of various types of inks [Peiponen et al. 2008], which are as follows: black 1.65 (ref. 1.6), blue & yellow 1.49 (ref. 1.53 – 1.54).

6 SUPPLEMENTAL RESULTS

Figure 2 presents additional renderings of samples acquired with our primary setup in the Eucalyptus Grove environment. Figure 4 presents renderings of samples acquired with our mobile setup in

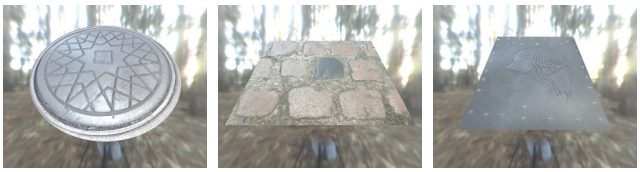

Fig. 4. Samples acquired with mobile setup rendered in Eucalyptus Grove.

Eucalyptus Grove. Figure 5 presents photograph-rendering comparisons under novel viewpoint and lighting conditions for some of the acquired samples. Here, the viewpoint and illumination data was not part of our capture set for reflectometry. Finally, Figure 6 presents a qualitative comparison of the reflectance and normal maps of the sketch book acquired using our mobile acquisition procedure against reference measurements with LCD illumination according to [Ghosh et al. 2009].

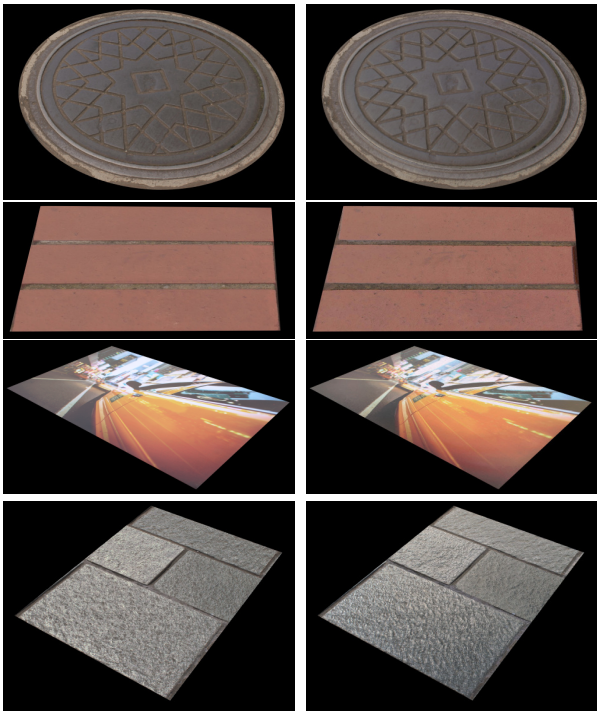

(a) Photograph (b) Rendering

Fig. 5. Comparison of renderings with photographs for a few of the acquired samples under a combination of a novel viewpoint and incident illumination.

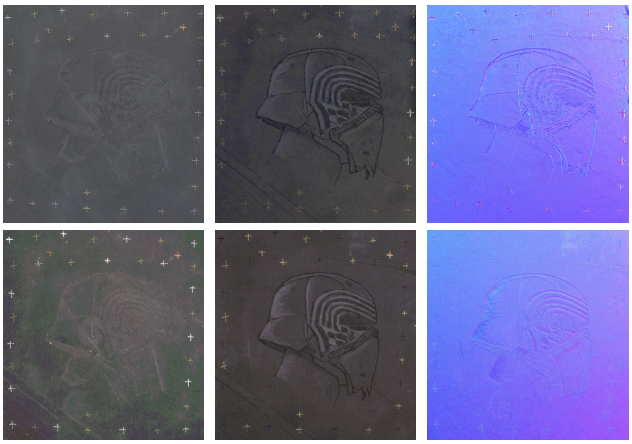

(a) Diffuse (b) Spec. R_0 (c) Surf. normal

Fig. 6. Comparison of reflectance maps of the sketch book acquired with our mobile setup (top row) against reference controlled measurement with LCD illumination (bottom row).

REFERENCES

Miika Aittala, Timo Aila, and Jaakko Lehtinen. 2016. Reflectance Modeling by Neural Texture Synthesis. *ACM Trans. Graph.* 35, 4, Article 65 (July 2016), 13 pages.

Miika Aittala, Tim Weyrich, and Jaakko Lehtinen. 2013. Practical SVBRDF Capture In The Frequency Domain. *ACM Trans. on Graphics (Proc. SIGGRAPH)* 32, 4 (2013).

Miika Aittala, Tim Weyrich, and Jaakko Lehtinen. 2015. Two-shot svbrdf capture for stationary materials. *ACM Transactions on Graphics* 34, 4 (2015), 110.

Gary Atkinson and Edwin R Hancock. 2006. Recovery of surface orientation from diffuse polarization. *Image Processing, IEEE Transactions on* 15, 6 (2006), 1653–1664.

E. Collett. 2005. *Field Guide to Polarization, SPIE Field Guides vol. FG05.* SPIE.

R. L. Cook and K. E. Torrance. 1982. A Reflectance Model for Computer Graphics. *ACM TOG* 1, 1 (1982), 7–24.

Craig Donner and Henrik Wann Jensen. 2006. A Spectral BSSRDF for Shading Human Skin. *Rendering techniques* 2006 (2006), 409–418.

Abhijeet Ghosh, Tongbo Chen, Pieter Peers, Cyrus A. Wilson, and Paul E. Debevec. 2009. Estimating Specular Roughness and Anisotropy from Second Order Spherical Gradient Illumination. *Comput. Graph. Forum* 28, 4 (2009), 1161–1170.

Abhijeet Ghosh, Tim Hawkins, Pieter Peers, Sune Frederiksen, and Paul Debevec. 2008. Practical Modeling and Acquisition of Layered Facial Reflectance. *ACM Transactions on Graphics* 27, 5 (Dec. 2008), 139:1–139:10.

Cong Phuoc Huynh, Antonio Robles-Kelly, and Edwin Hancock. 2010. Shape and refractive index recovery from single-view polarisation images. In *Computer Vision and Pattern Recognition (CVPR), 2010 IEEE Conference on.* IEEE, 1229–1236.

Achuta Kadambi, Vage Taamazyan, Boxin Shi, and Ramesh Raskar. 2015. Polarized 3D: High-Quality Depth Sensing with Polarization Cues. In *Proceedings of the IEEE International Conference on Computer Vision.* 3370–3378.

G.P. Können. 1985. *Polarized Light in Nature.* Cambridge University Press.

Daisuke Miyazaki, Takuya Shigetomi, Masashi Baba, Ryo Furukawa, Shinsaku Hiura, and Naoki Asada. 2012. Polarization-based surface normal estimation of black specular objects from multiple viewpoints. In *3D Imaging, Modeling, Processing, Visualization and Transmission (3DIMPVT), 2012 Second International Conference on.* IEEE, 104–111.

KE Peiponen, V Kontturi, I Niskanen, M Juuti, J Räty, H Koivula, and M Toivakka. 2008. On estimation of complex refractive index and colour of dry black and cyan offset inks by a multi-function spectrophotometer. *Measurement Science and Technology* 19, 11 (2008), 115601.

Pixel and Poly. 2017. Index of Refraction values (IOR) - For use with 3d modeling / rendering and animation applications. https://pixelandpoly.com/ior.html. (2017).

Bruce Walter, Stephen R Marschner, Hongsong Li, and Kenneth E Torrance. 2007. Microfacet models for refraction through rough surfaces. In *Proceedings of the 18th Eurographics conference on Rendering Techniques.* Eurographics Association, 195–206.